MNRAS **000**, 1–19 (2023) Preprint 24 May 2024 Compiled using MNRAS LATEX style file v3.0

Multi-wavelength Photometric Study of RR Lyrae Variables in the Globular Cluster NGC 5272 (Messier 3)

Nitesh Kumar,[1]★ Anupam Bhardwaj,[2] Harinder P. Singh,[1] Marina Rejkuba,[3] Marcella Marconi[4] and Philippe Prugniel[5]

Xingzhu Zou (邹星竹)
Yunnan University

2024-06-27

Outline

Part I Introduction

Introduction

- RR Lyrae stars are low mass ($0.5 \lesssim M/M_\odot \lesssim 0.8$), evolved stars (age $\gtrsim 10$ Gyr) located at the intersection of the horizontal branch and classical instability strip in the HertzsprungRussell diagram.
- Their well defined period-luminosity relation at infrared wavelengths makes them good standard candles.

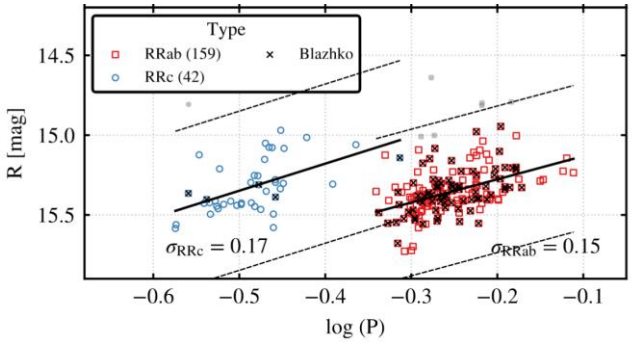

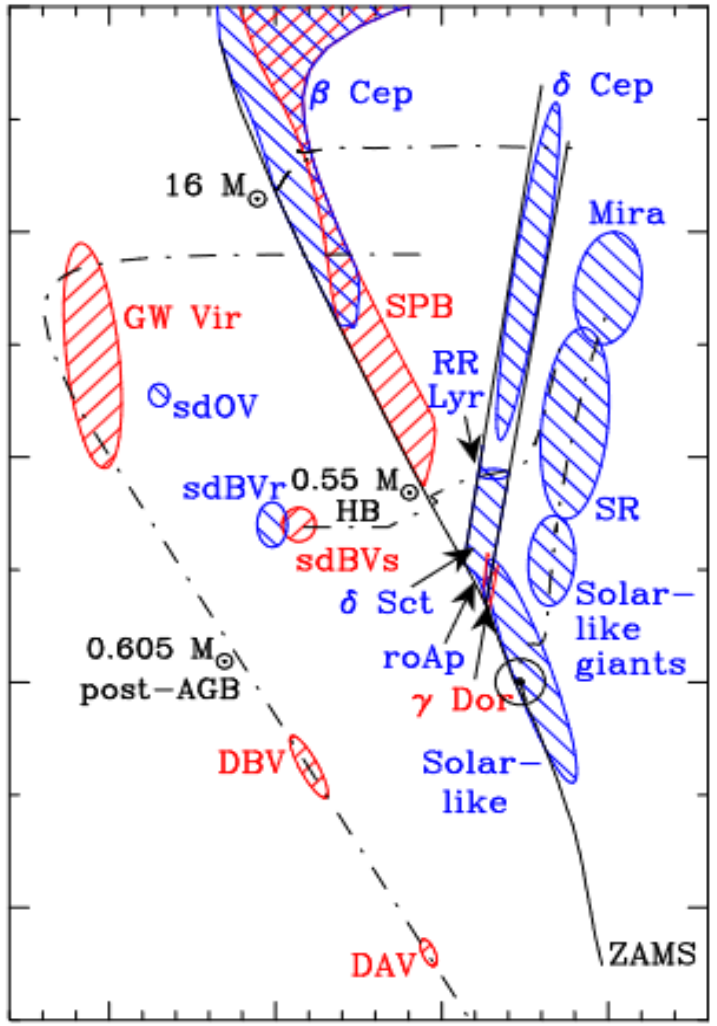

- they are valuable for studying stellar evolution and pulsation as well as for studying the structure, formation, and evolution of the Galactic halo.

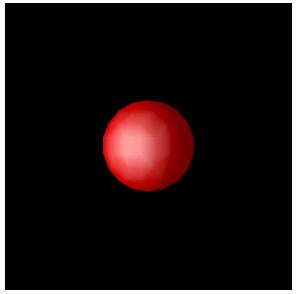

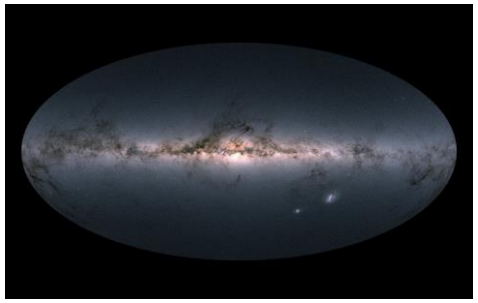

Introduction

- NGC 5272 (Messier 3 or M3, with R.A. (J2000) = 13h42m11s and Dec (J2000) = +28◦22′32″) is a globular cluster located approximately 11.9 kpc from the Galactic centre, about 10 kpc from the Sun, and around 9.7 kpc above the Galactic plane (Harris 1996).

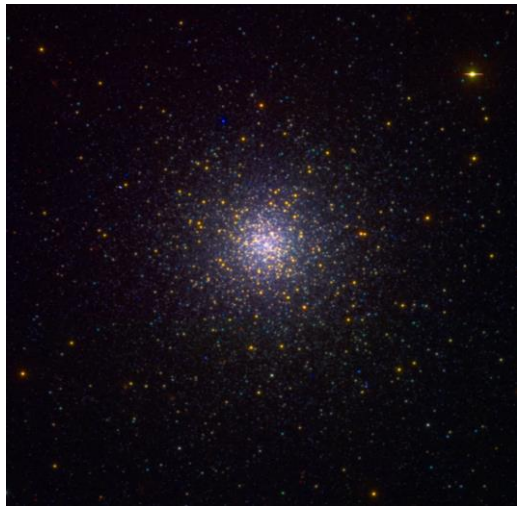

- This cluster has a population of approximately 240 RR Lyrae stars, many of which are fundamental mode RR Lyrae (RRab) stars. M3 is considered a mono-metallic cluster with a mean metallicity of [Fe/H] ~ -1.5 dex .

➢ A multi-band photometric study of the large sample of RR Lyrae in M3 using a vast dataset covering long time-baseline and spectral-coverage of observations will be useful to explore and analyse the pulsation properties of RR Lyrae stars in unprecedented detail.

➢ combined optical ($UBV\ RI$) and near-infrared (NIR, $JHKs$) photometry of RR Lyrae variables to investigate their pulsation properties such as period distributions and amplitude ratios. And the Period-Luminosity relations and Period-Wesenheit relations were derived .

Part II The data

The data

optical CCD images

- accurate, homogeneous, and consistently calibrated multi-band $UBVRI$ photometry for M3 based on 3140 optical CCD images obtained from public archives (Stetson et al. 2019).

- All images were preprocessed in a standard way, including bias subtraction and flat-fielding.
- The photometry and calibration were carried out using the DAOPHOT/ALLFRAME software.
- different standard filters (such as Sloan u, g, r, i, and Stroemgren b, y filters), which were transformed to standard Johnson/Kron-Cousins photometric $UBVRI$ bands/

- covers a sky area 57' × 56'
- spanning slightly over 35 years.

No.	Run	Dates	Telescope	Camera	n_U, n_B, n_V, n_R, n_I	n_u,n_b,n_y	n_u,n_g,n_r,n_i	Multiplex
1	cf84	1984 Jun 22	Maunakea CFHT 3.6m	RCA1	-, 1, 1, -, -	-, -, -	-, -, -, -	—
2	kp36	1985 Jun 12	KPNO 0.9m	RCA	-, 4, 4, -, -	-, -, -	-, -, -, -	—
3	kp4m	1985 Jun 16-18	KPNO 4m	RCA	-, 6, 5, -, -	-, -, -	-, -, -, -	—
4	cf85	1985 Jun 20-24	Maunakea CFHT 3.6m	RCA1	-, 10, 10, -, -	-, -, -	-, -, -, -	—
5	jvw	1986 Mar 29-Apr 09	La Palma INT 2.5m	RCA	4, 6, 8, 9, 6	-, -, -	-, -, -, -	—
6	km	1986 May 08	La Palma INT 2.5m	RCA	-, 1, 2, -, -	-, -, -	-, -, -, -	—
7	c91ic41	1991 Apr 08	Maunakea CFHT 3.6m	lick1	-, 2, 2, -, 2	-, -, -	-, -, -, -	—
8	cf91	1991 Jul 06-07	Maunakea CFHT 3.6m	Lick2	-, 2, 2, -, -	-, -, -	-, -, -, -	—
9	saic	1992 May 25	Maunakea CFHT 3.6m	HRCam/saic1	-, -, 16, 15, -	-, -, -	-, -, -, -	—
10	h92ic1	1992 May 27	Maunakea CFHT 3.6m	HRCam	-, 7, -, -, -	-, -, -	-, -, -, -	—
11	cf92	1992 Jun 08-09	Maunakea CFHT 3.6m	RCA4	-, 3, -, -, -	-, -, -	-, -, -, -	—
12	bolte	1994 Apr 13-16	KPNO 2.1m	t1ka	-, -, 30, -, 31	-, -, -	-, -, -, -	—
13	cf94	1994 Jun 06	Maunakea CFHT 3.6m	Loral3	-, 4, -, -, 4	-, -, -	-, -, -, -	—
14	jka	1995 Mar 27	La Palma INT 2.5m	TEK3	-, 3, 8, -, -	-, -, -	-, -, -, -	—
15	bond9	1997 May 08-10	KPNO 0.9m	t2ka	-, 4, 4, -, 4	-, -, -	4, -, -, -	—
16	arg	1997 May 31	La Palma JKT 1m	TEK2	-, -, 3, -, 6	-, -, -	-, -, -, -	—
17	bond11	1998 Mar 21-22	KPNO 0.9m	t2ka	-, 9, 9, -, 9	-, -, -	1, -, -, -	—
18	int9804	1998 Apr 12	La Palma INT 2.5m	WFC	-, 3, -, 4, -	-, -, -	-, -, -, -	—
19	dmd	1998 Jun 24	La Palma JKT 1m	TEK4	-, -, 2, -, 2	-, -, -	-, -, -, -	—
20	tng2	2000 Feb 04	La Palma TNG 3.6m	OIG	2, 2, 2, -, -	-, -, -	-, -, -, -	x 2
21	int0005	2000 May 24-28	La Palma INT 2.5m	WFC	-, 3, 3, -, -	-, -, -	-, -, -, -	x 4
22	jun00	2000 Jun 04	Maunakea CFHT 3.6m	CFH12K	-, -, 2, -, -	-, -, -	-, -, -, -	x 12
23	cf0102	2001 Feb 16-17	Maunakea CFHT 3.6m	CFH12K	-, 15, 18, -, 12	-, -, -	-, -, -, -	x 12

The data

Identification of variable stars

- The identification of RR Lyrae stars in the M3 globular cluster was accomplished using the reference list compiled by Clement et al.

Table 2. Optical time-series photometry of RR Lyrae stars in M3 cluster. The complete table can be accessed online in machine-readable format.

Id	Run Name	Image Name	Band	Filter Flag	HJD	mag	σ_{mag}	χ	Sharp
V1	bond9	obj1801	U	b	2450576.8756	15.835	0.0446	1.55	0.056
V1	bond9	obj3001	U	b	2450577.8346	15.320	0.0199	1.66	0.010
V1	bond9	obj4201	U	b	2450578.8378	16.346	0.0347	2.26	0.106
V1	bond9	obj4205	U	b	2450578.8563	15.673	0.0256	2.23	0.067
V1	bond11	obj6801	U	b	2450894.9046	15.370	0.0215	1.58	0.036
V1	int1202	1m3U30a_4	U	a	2455979.6201	15.689	0.0136	1.52	0.170
⋮	⋮	⋮							
V1	c91ic41	111709o							229
V1	c91ic41	111710o	B	a	2458354.9777	15.611	0.0118	5.14	0.069
V1	bond9	obj1802							103
⋮	⋮	⋮							

total number of RR Lyrae stars 238.

- 178 RRab stars
- 49 RRc stars
- 11 double/multi-mode (RRd) variables
- 90 were Blazhko variables of this group.

Blazhko effect :the light curves' amplitude and phase modulations over a timescale significantly longer than their primary pulsation period.

RRab star

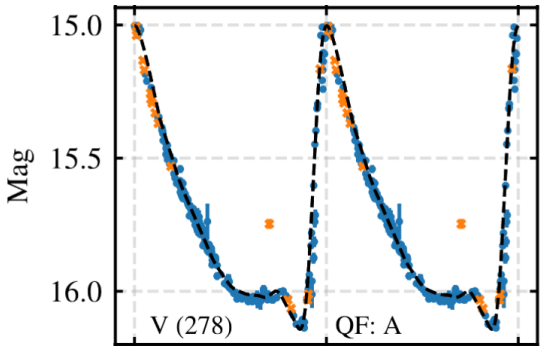

RRc star

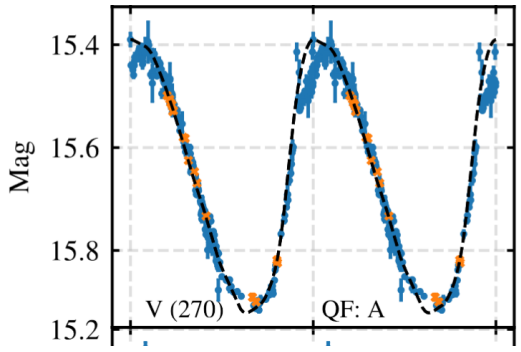

non-Blazhko stars

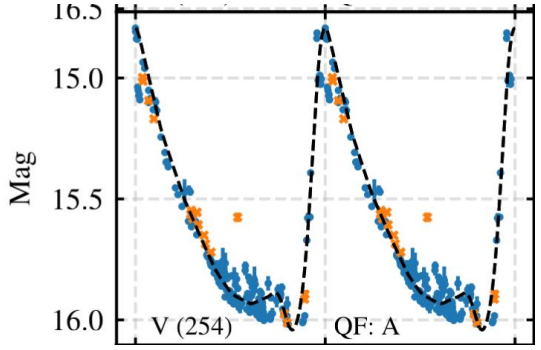

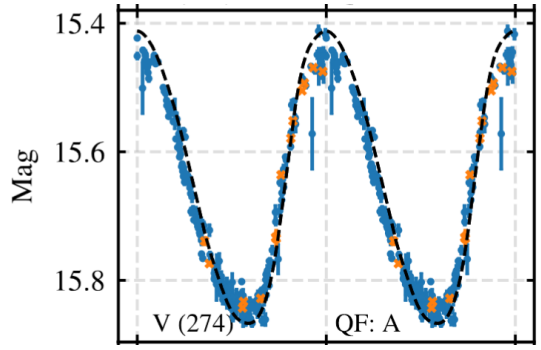

Blazhko stars

Part III
Determination of pulsation properties

Determination of pulsation properties

Period determination and distribution

Multi-band Lomb Scargle (MBLS) algorithm method utilizes a shared base model and combines residuals from individual fits to determine the overall period of the data across multiple filter pass bands.

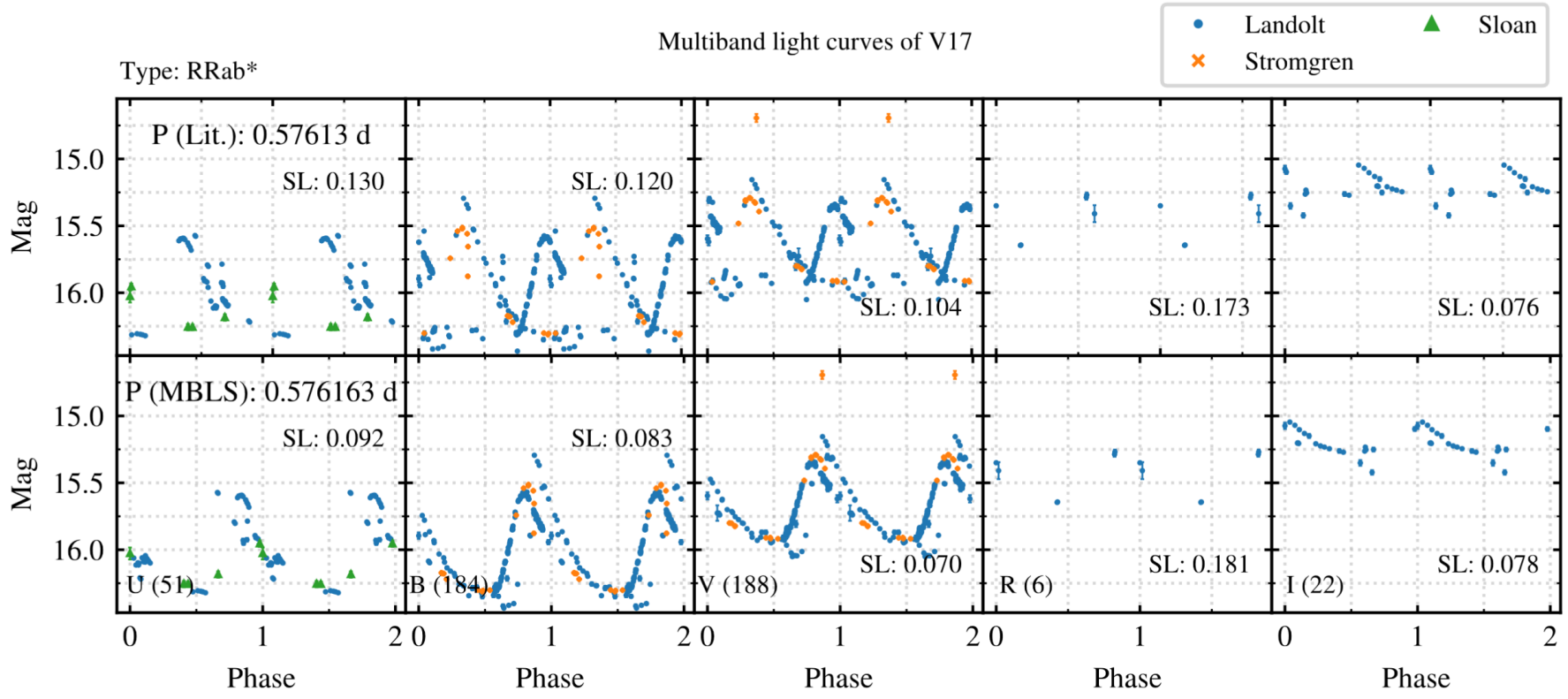

Determination of pulsation properties

To assess the consistency, validity, and accuracy of the derived periods:

- periods obtained through the Multi-Band Lomb Scargle (MBLS) method and those reported by literature
- smaller string length per unit phase usually indicates a better period fitting.

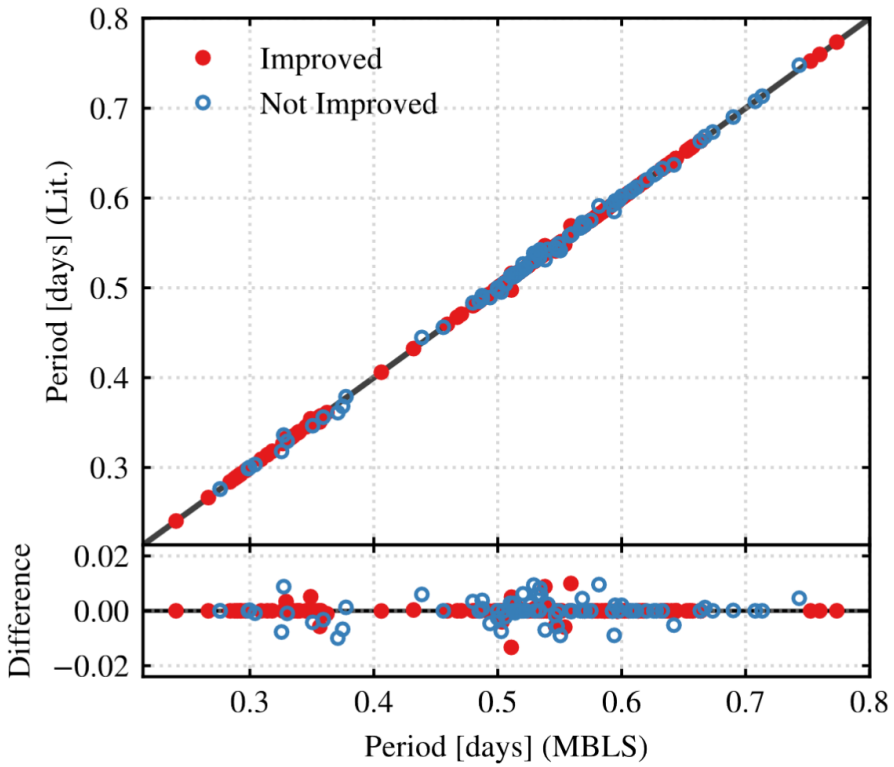

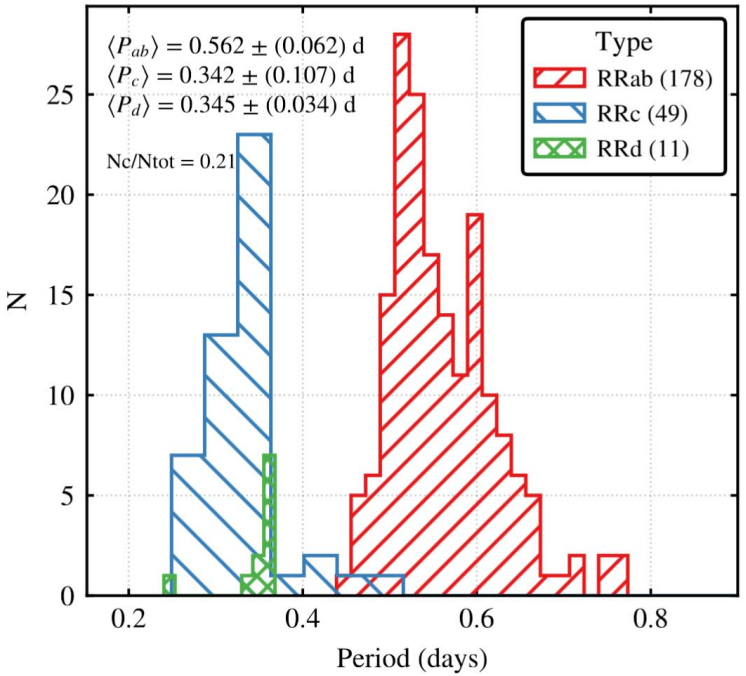

The mean period of M3's RRab stars:0.562 days
The mean period of M3's RRc stars :0.342 days

Determination of pulsation properties

Template fitting

- the templates generated by Sesar et al. (2009)
- fundamental parameters as input : period, the epoch of maximum light, and amplitude ratio.
- minimised the $\chi 2$ deviation between the actual magnitude measurements (m) and the template fit magnitudes ($m$fit).

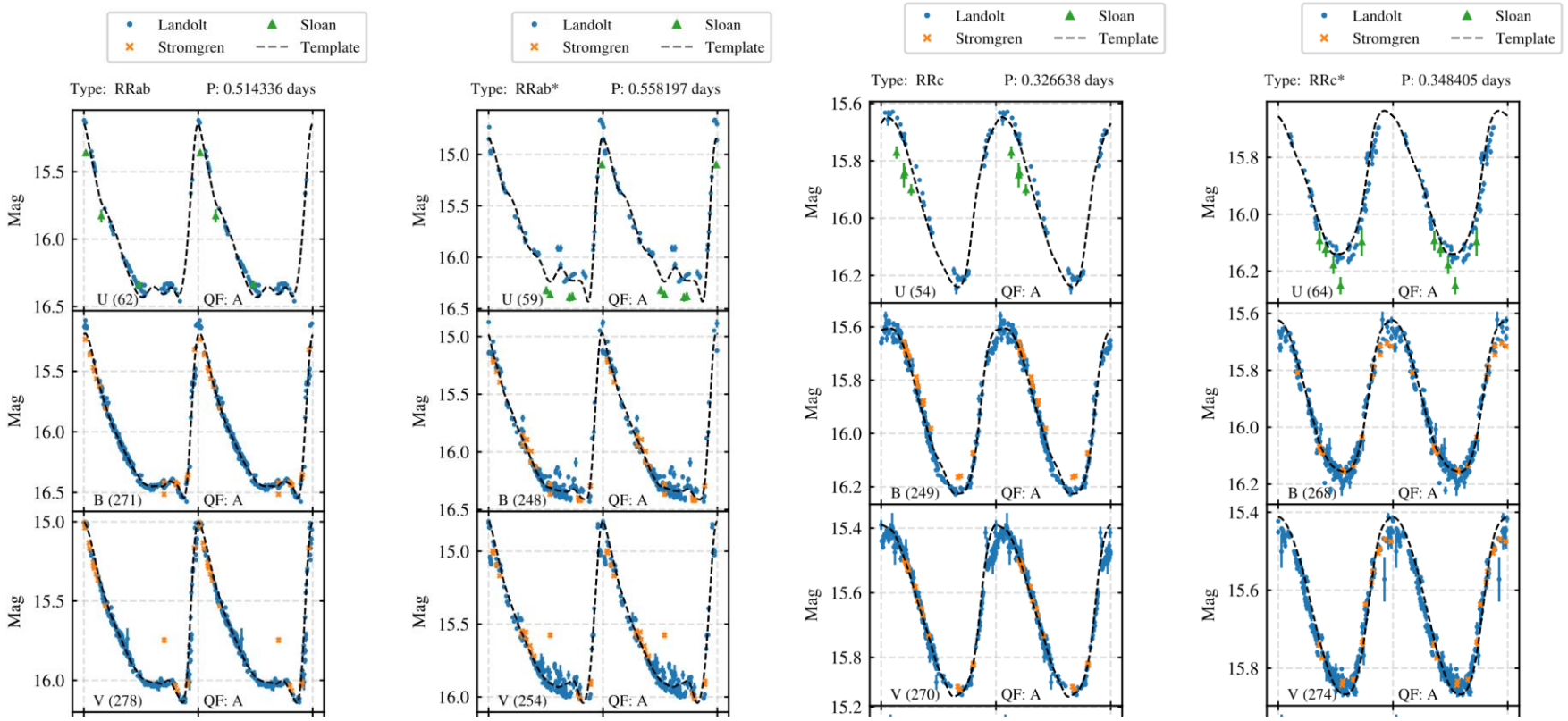

solve for the mean magnitude, amplitude, and a phase offset simultaneously.

Determination of pulsation properties

Template fitting

Table 3. Properties of RR Lyrae variables in M3, including their identification (Id), period, intensity averaged mean magnitudes, and amplitudes in the U, B, V, R, and I filters. The Oosterhoff classification, Blazhko variability, and the quality flags (QF) are also provided. The QF values are given in a sequence for the $UBVRI$ filter bands, respectively. The complete table can be accessed online in a machine-readable format.

Id	RA[c]	Dec[c]	Type	Blazhko[b]	Period (days)	Oo Type[b]	<U> mag	A_U mag	<B> mag	A_B mag	<V> mag	A_V mag	<R> mag	A_R mag	<I> mag	A_I mag	QF (UBVRI)
V1	13:42:11.12	+28:20:33.8	RRab	-	0.520590[b]	OoI	15.78	1.31	15.90	1.38	15.62	1.18	15.41	0.81	15.17	0.68	AAAAA
V3	13:42:15.71	+28:21:41.8	RRab	Bl	0.558197[a]	OoII	15.70	1.59	15.85	1.44	15.53	1.25	15.34	0.86	15.09	0.77	AAAAA
V5	13:42:31.29	+28:22:20.7	RRab	Bl	0.505834[a]	OoI	15.97	0.94	15.90	1.42	15.58	1.26	15.55	0.56	15.16	0.83	AAAAA
V6	13:42:02.08	+28:23:41.6	RRab	-	0.514336[a]	OoI	15.97	1.29	16.00	1.36	15.68	1.14	15.52	0.90	15.24	0.73	AAAAA
V7	13:42:11.09	+28:24:10.2	RRab	Bl	0.497423[a]	OoI	15.97	1.43	15.88	1.47	15.55	1.25	15.52	0.92	15.20	0.74	ABBAA
⋮	⋮	⋮	⋮	⋮	⋮	⋮	⋮	⋮	⋮	⋮	⋮	⋮	⋮	⋮	⋮	⋮	⋮
V270n	13:42:11.95	+28:23:32.7	RRab	Bl	0.625850[b]	-	15.77	0.64	15.73	0.95	15.43	0.87	15.28	0.42	14.92	0.44	ABBAA
V271	13:42:12.18	+28:23:17.6	RRab	-	0.632800[c]	-	16.05	0.88	16.06	0.86	15.66	0.64	15.44	0.15	15.06	0.38	AAAAA
V290	13:42:21.30	+28:23:45.0	RRd	-	0.240413[a]	-	15.91[†]	0.25[†]	15.85[†]	0.54[†]	15.67[†]	0.07[†]	15.53[†]	0.22[†]	15.38[†]	0.30[†]	——
V292	13:42:11.18	+28:21:54.0	RRc	-	0.296543[a]	-	15.81	0.36	15.77	0.37	15.61	0.29	15.45	0.21	15.32	0.21	AAAAA
V299	13:41:18.85	+28:01:57.0	RRc	-	0.249200[c]	-	15.93[†]	-	15.80[†]	-	15.60[†]	-	-	-	15.42[†]	-	-

All the magnitudes were corrected for Galactic extinction $E\ (B-V) = 0.013$ with the conversion factors adopted from Schlegel et al. (1998)

Part Ⅳ Determination of Relations and Distance

Determination of Relations and Distance

Period-Luminosity (PL) Relations

RR Lyrae exhibit a well-defined Period-Luminosity relationship (PLR) in near-infrared wavelength bands

$$m_\lambda = b_\lambda \log(P) + a_\lambda,$$

$$\log P_{FU} = \log P_{FO} + 0.127,$$

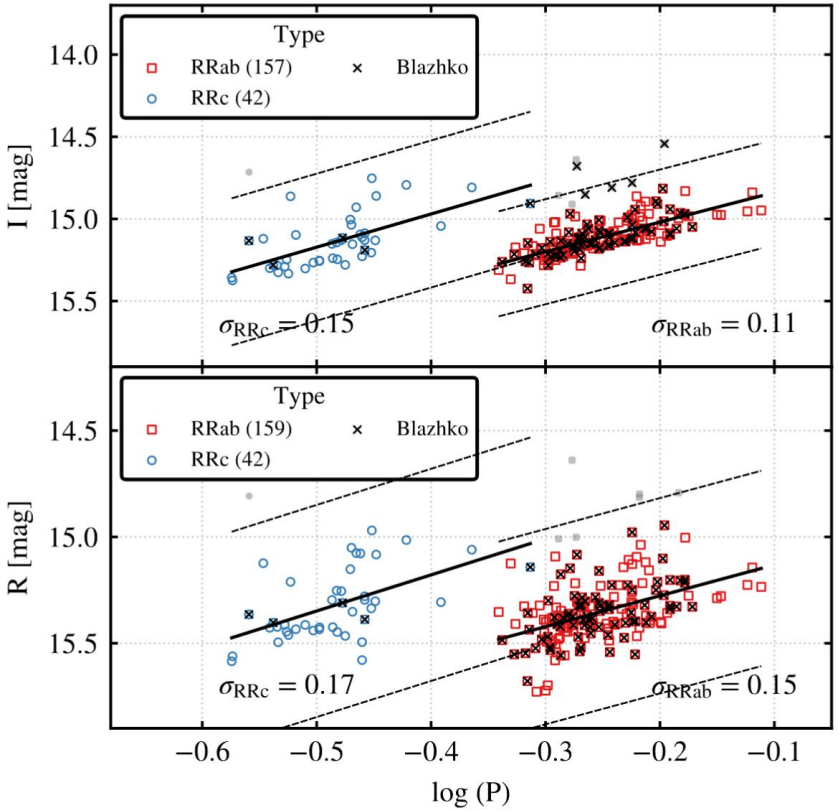

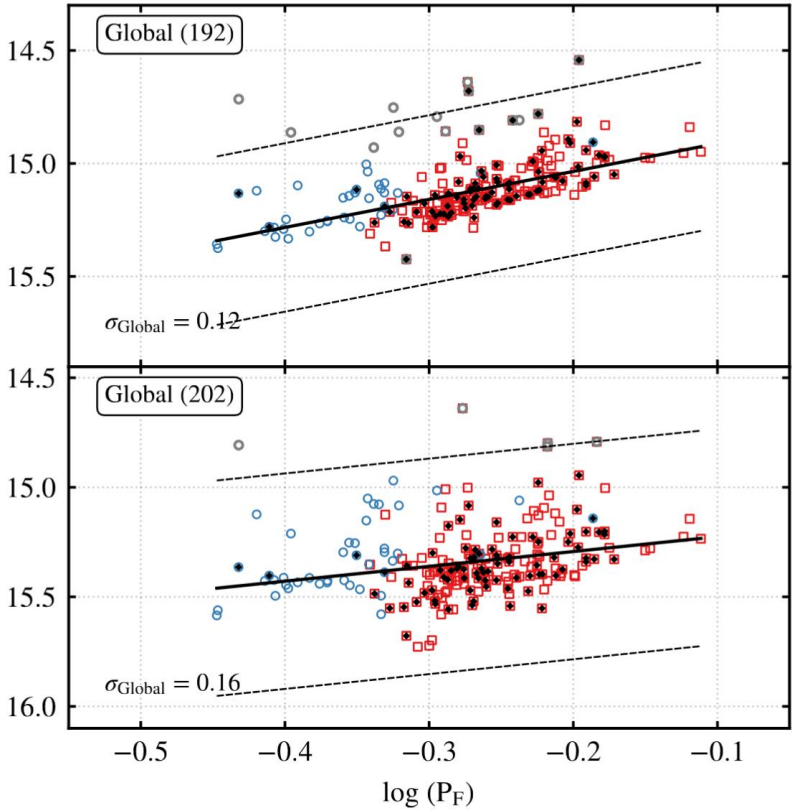

The scatter (rms) in the PLRs is a consequence of the intrinsic width of the instability strip in temperature. It may also arise due to the metallicity spread of the RR Lyrae in clusters and the uncertainties in extinction correction.

Determination of Relations and Distance

Period-Wesenheit (PW) Relations

Wesenheit index is defined as a combination of multiple passband magnitudes of a star in a way that effectively eliminates the impact of reddening.

$$W(X, Y) = M_X - \xi(M_X - M_Y),$$

coefficient of the color term— ξ—is the ratio between the selective absorption in the X band and the color excess in the adopted color.

They adopted the same Wesenheit magnitudes constructed for theoretical models in Marconi et al. (2015):

V - 3.06(B - V) [mag] I - 1.38(V - I) [mag]

$$m_\lambda = b_\lambda \log(P) + a_\lambda,$$

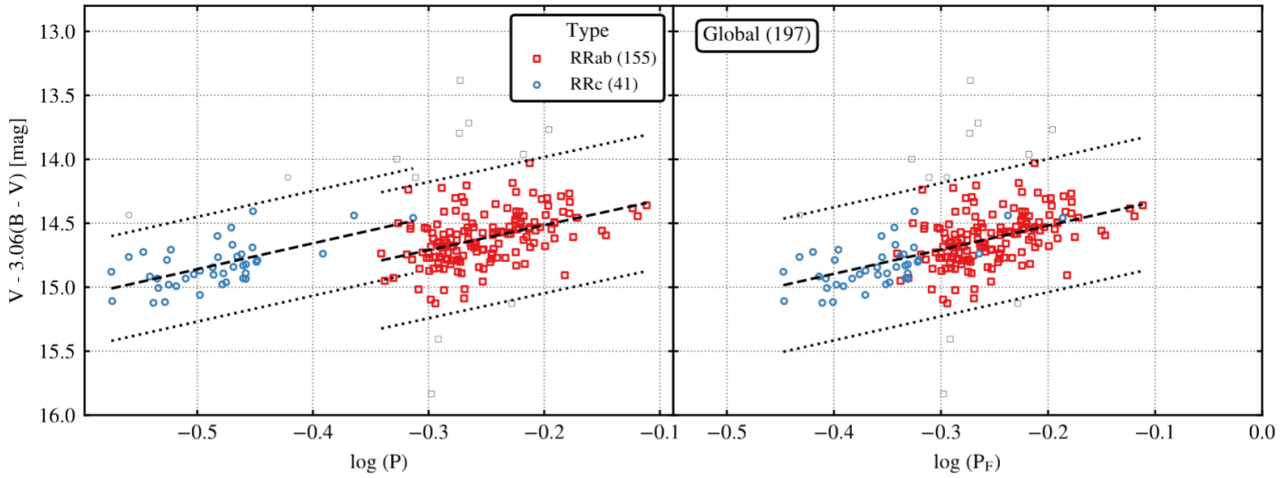

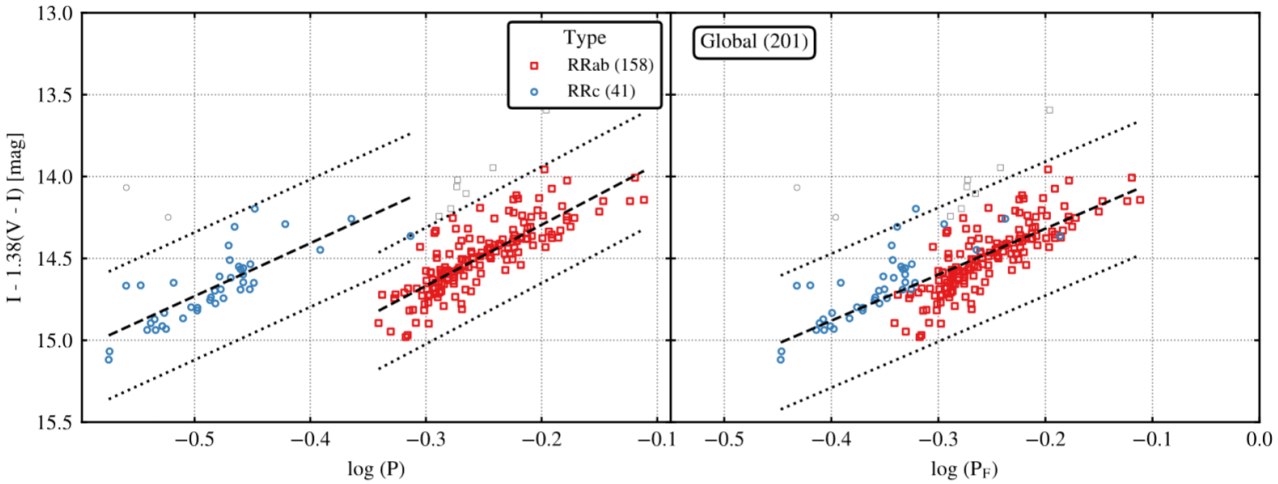

Determination of Relations and Distance

Using the derived PW relations for FU(Rrab), FO(RRc), and the global sample of stars, they calculated the distances to each RR Lyrae star and then determined the mean distance to the M3 cluster.

Using the metal-dependent PW(I, $V-I$) relation and adopting [Fe/H] = −1.53 dex, Employing the theoretical relations from Marconi et al. (2015):

distance moduli (μ) to M3 :

15.05 ± 0.06 (statistical) ± 0.08 (systematic) mag for FU

15.01 ± 0.02 ± 0.28 mag for FO

15.05 ± 0.03 ± 0.06 mag for the global sample.

- statistical error :accounts for the dispersion in the distribution of individual RR Lyrae star distance moduli.
- systematic error: reflects the discrepancy between the theoretical and semi-empirical calibration of the PWrelations.

μ = 15.03 ± 0.17(syst.)±0.04

The results were compared with those from other studies, showing good agreement in both optical and near-infrared photometric determinations.

Part V Conclusions

Conclusions

this study on the M3 globular cluster utilized a large photometric dataset spanning 35 years to investigate the pulsation properties of its RR Lyrae population.

By analyzing light curves at multiple filter bands and employing the Multi-Band Lomb Scargle algorithm, accurate period measurements were obtained for a significant number of stars.

Template fitting and multi-band photometric data were used to study the instability strip and filter out outlier stars. The study confirmed the classification of RRab and RRc stars using Bailey's diagram and observed general agreement with literature values for luminosity amplitude ratios.

Period-Luminosity and Period-Wesenheit relations were derived for different bands, showing good agreement with theoretically predicted relations. The distance modulus of M3 was determined to be consistent with previous literature, with values obtained using metal-dependent Wesenheit magnitudes.

Thank you!

Thank you for your attention!